Equilibrium polymerization in sulphur: Monte Carlo simulations with a density functional based force field

P. Ballone[1,2] **and R. O. Jones**[1]

[1] Institut für Festkörperforschung, Forschungszentrum Jülich, D-52425 Jülich
E-mail: {p.ballone, r.jones}@fz-juelich.de

[2] Dipartimento di Fisica, Università di Messina, I-98166 Messina, Italy

The equilibrium polymerization of sulphur is investigated by a combination of density functional (DF) computations for gas-phase molecules and Monte Carlo simulations for the reacting liquid phase. The DF calculations provide a detailed description of the elementary processes leading to polymerization, and the results for the cohesive energy, structural and vibrational properties of sulphur chains and rings provide input parameters for a semi-empirical atomistic model. Monte Carlo simulations account for many-atom effects and for thermal averaging. The results allow us to estimate the zero-pressure polymerization temperature of sulphur at $T_f = 450 \pm 20$ K, in good agreement with experiment ($T_f^{exp} = 432$ K). The simulation results reproduce qualitative changes in the experimental radial distribution function, and the estimates for thermodynamic properties agree well with experimental data.

1   Introduction

Polymeric molecules are basic constituents of biological systems, and organic polymers represent an important class of technological materials. It is not surprising that much effort has been devoted to identify, control and optimize the chemical and thermodynamic conditions needed to produce long chain molecules from simpler species (monomers, oligomers, etc.). Much progress has been achieved in theory and experiment, but our understanding of polymerization is far from complete.

Computational methods, particularly simulations, are playing an increasing role in the investigation of polymerization. The improvement of computing facilities and methods allow us to analyze the elementary processes leading to polymerization with unprecedented resolution, while simulation methods provide an effective way to account for many-body and statistical mechanics effects. An example of the range of methods required to describe these phenomena, as well as the quality of the results, is provided by our recent study of sulphur polymerization. We outline this work here.

Elemental sulphur is known for the large number of solid allotropes it forms at relatively low temperature and pressure.[1] At the melting point $T_m = 386$ K, these forms give way to a liquid phase comprising S_8 molecules with small concentrations of S_n rings with $6 \leq n \leq 23$.[2] At $T_\lambda = 432$ K, sulphur undergoes a liquid-liquid transition (λ transition), usually interpreted as the ring opening polymerization (ROP) of S_8. Polymerization is reversible, takes place under equilibrium conditions, and is revealed by a change of color, anomalies in the specific heat and volume expansion coefficient, and a dramatic increase of viscosity.[3]

This transformation is investigated here by a combination of density functional (DF) computations and Monte Carlo simulations. The agreement between theory and available

experimental data provides support for both the computations underlying the potential energy determination, as well as the atomistic model and the Monte Carlo simulation of the reacting system.

2 Density functional studies of structure and reactivity of sulphur molecules

Sulphur rings with up to 18 atoms and chains with up to 10 atoms have been investigated by DF computations using both an atomic-like (Gaussian) basis set and a plane wave - molecular dynamics implementation. Both approaches lead to large scale computations requiring a supercomputer. We have focused on trends in the geometry and energy differences among different isomers and between rings and chains. The number of isomers increases rapidly with increasing molecular size for both rings and chains, and the additional covalent bond makes rings more stable than the corresponding chains. The cohesive energy of the most stable ring isomer shows peaks at $n = 8$ and $n = 12$. Strain destabilizes rings with less than 8 atoms, while for $n > 12$ the size dependence of the cohesive energy is reduced to a slight even/odd alternation.

The primary aim of the DF study was to provide the input parameters for a model of liquid sulphur and its polymerization. For this reason, the repulsive interaction between two S_8 singlet rings has been compared with the energy changes occurring when an S_8 triplet diradical approaches an S_8 ring. As shown in Fig. 2, the ring opens in the latter case, leading to a diradical chain of 16 atoms. The calculated energy barrier is at most 5.4 kcal/mol. Moreover, structural and energy parameters are readily transferable between molecules, thus greatly simplifying the task of building an atomistic model. There is a relatively narrow range of bond angles and a clear relation between the length of a bond in a chain or ring and the corresponding dihedral angles. Trends in the vibrational frequencies are also quite consistent: The ring structures have maximum frequencies that are typically below $500\,\mathrm{cm}^{-1}$, while terminal group of chains have frequencies above $600\,\mathrm{cm}^{-1}$. These results provide a basis for building an energy model of reacting condensed sulphur phases.

3 Monte Carlo simulations of polymerization

3.1 The model

The potential energy of the system as a function of the atomic coordinates is modeled by a potential comprising bonded (U_b) and non-bonded (U_{nb}) interactions. The bonded interactions include stretching, bending and torsion contributions, while non-bonding interactions are described by a Lennard-Jones (LJ) potential. The free parameters in the potential are varied in order to fit the DF results for the energy and structure of small rings, as well as the experimental volume and compressibility of the crystal phase. Most atoms in our simulations have covalent bonds to two neighbors, with a small (and temperature dependent) fraction adopting an unsaturated configuration with a single covalent bond.

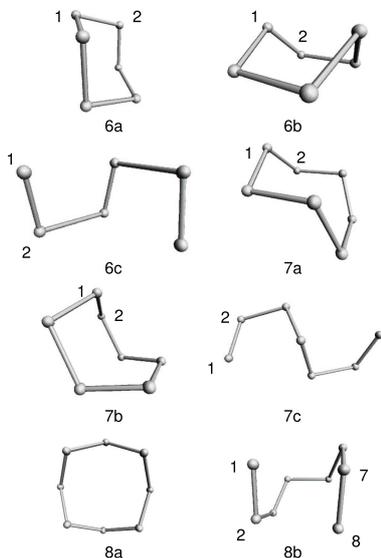The polymerization of sulphur takes place in two steps:
(1) Initiation:

$$cyclo - S_8 \longrightarrow chain - S_8^{\cdot\cdot}$$
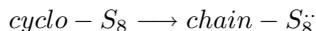
Figure 1. Structures of S_6, S_7, and S_8 isomers. Isomers are ordered alphabetically according to energy, beginning with the most stable.
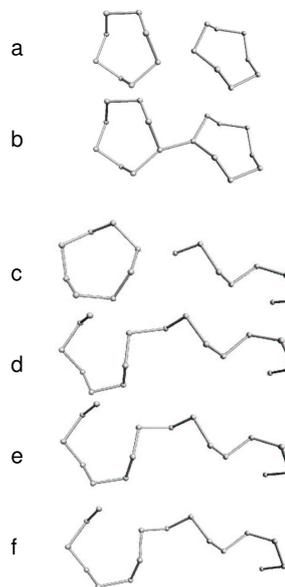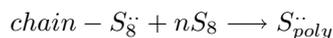

Figure 2. (a-b) Reaction of two S_8 rings, (c-f) reaction of an S_8 chain (triplet) with an S_8 ring. The shortest distances between the units are (a) 2.53 Å, (b) 2.32 Å, (c) 2.58 Å, (d) 2.38 Å, (e) 2.28 Å, (f) 2.13 Å.

(2) Propagation:

$$chain - S_8^{\cdot\cdot} + nS_8 \longrightarrow S_{poly}^{\cdot\cdot}$$

The enthalpies of the initiation (ΔH_I) and propagation (ΔH_P) step have been estimated by Tobolsky and Eisenberg[4] to be 32.8 and 3.17 kcal/mol, respectively. A more recent estimate of the propagation enthalpy yields $\Delta H_P = 4.5$ kcal/mol.[5] To reproduce these effects we introduce bond breaking and formation, which are assumed to be discontinuous processes; each pair of atoms is either bonded or not bonded at a given time, and their bonding state (represented by an independent binary variable) is not determined uniquely by the interatomic distance. The energy ΔE_b is required to break a bond and is released on bond formation.

Broken bonds open the way to propagation, which takes place via a bond switching mechanism involving one unsaturated atom (see Fig. 3). The corresponding energy barrier depends on the interaction of the radical atom with all others and has been tuned to reproduce the DF results for the reactivity of rings with chains.

3.2 Method

The Monte Carlo (MC) method is used for simulating the polymerization reaction in the NPT ensemble at $P = 0$. The MC procedure includes different types of moves: Single
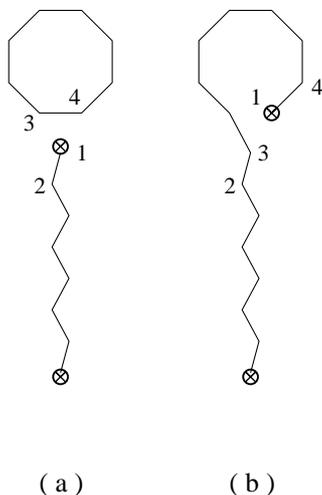
Figure 3. Schematic view of bond interchange mechanism. The circles with a cross indicate unsaturated atoms.

atom moves are attempted using standard Metropolis MC, and whole molecule moves are also attempted. Bond breaking and formation are attempted with the same frequency as single atom moves, but their acceptance probability is orders of magnitude smaller. In principle, bond breaking and formation are sufficient to establish equilibrium with respect to the bonding configuration, but the kinetics are exceedingly slow for realistic choices of the bond energy ΔE_b. Bond switching processes lead to equilibrium with a significantly lower energy barrier.

Values of ΔE_b lower than 15 kcal/mol lead to an unrealistically large number of broken bonds for $T \geq 450$ K and a significant increase in the system volume. If, however, the number of broken bonds in the simulation cell decreases below the critical number of one for $\Delta E_b > 21$ kcal/mol and $T \sim 500$ K, the system does not reach equilibrium. For accessible values ($15 \leq \Delta E_b \leq 21$ kcal/mol) the results of the simulation depend significantly on ΔE_b, and we have performed a sequence of simulations spanning the interval $450 \leq T \leq 800$ K for $\Delta E_b = 15$, 18, 20 and 21 kcal/mol. This provides a basis for the extrapolation of the results to the physical value $\Delta E_b \sim 35$ kcal/mol.

Convergence with respect to the bond configuration has been monitored by computing the probability distribution as a function of cluster size. Full equilibration requires from 10^6 single particle moves per atom at the highest temperatures to 10×10^6 moves per atom at the lowest. The averages reported below have been computed over runs of length equal to that of the equilibration stage under the same conditions. We have noted that the number of attempts of bond interchange and bond breaking/formation attempts is equal to the total number of single atom moves, i.e., for either equilibration and production runs it ranges from 2048×10^6 at the highest temperatures, to 2048×10^7 at the lowest temperatures.
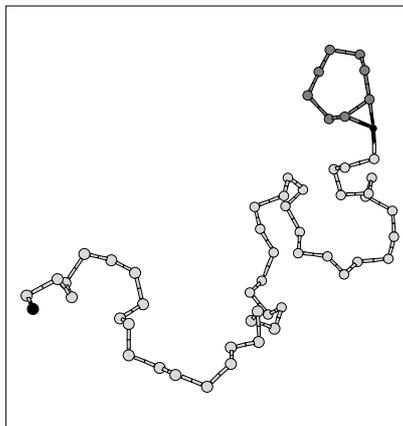
4

Figure 4. Snapshot of an activated complex (*tadpole*) leading to bond interchanges. The complex consists of an S_8 ring (dark gray) and an open chain (light gray). Unsaturated atoms are black.

3.3   Results

Every simulation began from a liquid sample comprising S_8 rings, equilibrated by a constant pressure simulation at fixed bonding topology. A long sequence of MC steps is required before the first broken bond appears within the system. With one or two exceptions (in more than 20 cases) the first pair of unsaturated atoms does not recombine before taking part in bond interchanges, thus beginning the propagation stage of polymerization.

Bond interchanges occur preferentially at atomic configurations in which one unsaturated chain head approaches two saturated atoms belonging to a ring (see Fig. 4) or another chain. The role of the threefold-coordinated unsaturated atoms at the center of these active sites was noted in earlier work,[6] where configurations similar to those of Fig. 4 were referred to as *tadpoles*. The MC kinetics of the polymer growth can be monitored by plotting the number N_L of atoms belonging to molecules (chains or rings) with more than L atoms. An example is N_{24}, shown in Fig. 5(a) for $T = 750$ K and $\Delta E_b = 21$ kcal/mol.

The growth of the polymer phase is accompanied by an increase in the average potential energy of the system (see Fig. 5 (b)). This is not a transient effect due to the reaction, but an equilibrium property of the polymer, which is stable despite its energy disadvantage with respect to the molecular phase. A detailed analysis of the thermodynamic data, and of their dependence on temperature and ΔE_b allows us to estimate $\Delta H_P(T = 450\ K) = 242$ K/atom, equal to 3.85 kcal/mol S_8, in fair agreement with the estimate ($\Delta H_P = 4.5$ kcal/mol) based on experimental data.[5]

A *polymeric molecule* is defined here as a chain or ring with more than 24 atoms, so that the equilibrium value of N_{24} is a measure of the polymerized fraction. There is a maximum in the polymer fraction at a temperature T_{max} that grows with increasing ΔE_b (see Fig. 6). Further temperature increase leads to a significant decrease in N_{24}, because the exponential increase in the number of unsaturated atoms produces many shorter seg-
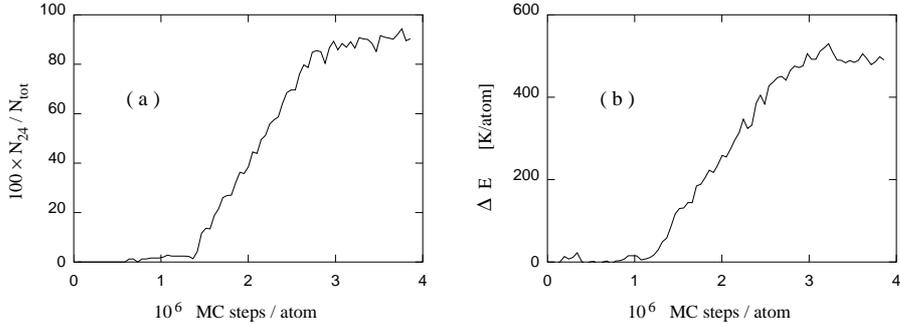
Figure 5. Evolution of properties as a function of the number of MC steps during polymerization at $T = 750$ K, $\Delta E_b = 21$ kcal/mol. (a) Percentage of atoms belonging to molecules with more than 24 atoms. (b) Average potential energy per atom. The zero of the energy is the average potential energy of the molecular S_8 phase at the same temperature.

ments. The decrease of the polymerization degree at $T < T_{max}$ is apparently due to the progressive stabilization of S_8 rings, whose potential energy advantage with respect to the polymer phase becomes more important at low T. Other small rings contribute little to the total system mass at all T.

The variation of the average length of polymeric molecules as a function of T and ΔE_b reflects the number of broken bonds and the polymer fraction N_{24} (see Fig. 7). Molecules with more than 24 atoms are almost all chains, whose number at any time is equal to the number of broken bonds (or half of the number of unsaturated atoms). Moreover, the number of chains with less than 24 atoms is very small in well polymerized samples (i.e., where N_{24} is higher than 50%). The average value of N_{24} is then approximately equal to the average length of polymeric molecules times the average number of broken bonds. The average length $\langle L \rangle$ will then decrease faster than the polymer fraction for $T \geq T_{max}$, reflecting the decrease of N_{24} and the increase of the average number of chains with increasing T. $\langle L \rangle$ will peak at a temperature $T_{max}^{\langle L \rangle}$ somewhat lower than T_{max}. On cooling below $T_{max}^{\langle L \rangle}$, $\langle L \rangle$ will decrease more slowly than N_{24}, since the decrease in the polymer fraction with decreasing T is partly compensated by the decrease in the number of unsaturated atoms (and chains).

The equilibrium size distribution of the sulphur molecules (chains or rings) is characterized by the function $p(L)$, defined as:

$$p(L) = n(L) / \sum_{L=1}^{\infty} n(L) \tag{1}$$

where $n(L)$ is the average number of molecules whose size is L. A typical result for a polymerized sample is shown in Fig. 8. A sharp peak is apparent at $L = 8$ for all T in both
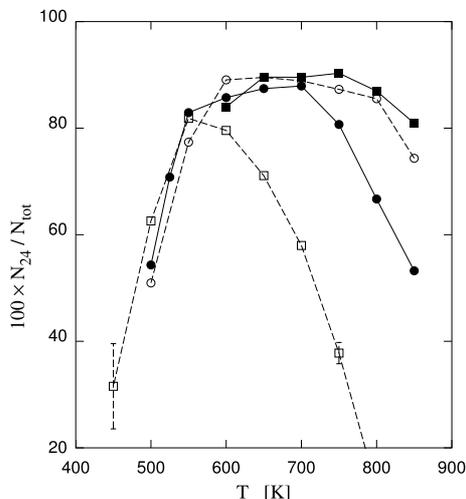
Figure 6. Average value of N_{24} as a function of T. Empty squares: $\Delta E_b = 15$ kcal/mol; solid dots: $\Delta E_b = 18$ kcal/mol; empty circles: $\Delta E_b = 20$ kcal/mol; full squares: $\Delta E_b = 21$ kcal/mol. Representative error bars are shown. Lines are a guide to the eye.

$p(L)$ and $P(L)$. For larger sizes, $p(L)$ is reproduced well by a Zimm-Schulz distribution:

$$p(L) \propto L^{\gamma-1} \exp\left[-\gamma L/\langle L \rangle\right] \tag{2}$$

with an exponent $\gamma = 1.1$ that is almost independent of T and ΔE_b. The simpler function $p(L) \propto \exp\left[-L/\langle L \rangle\right]$ provides a fit whose chi-square is almost as good. The peak of $p(L)$ at $L = 8$ is not an artifact of incomplete equilibration of the original population of S_8 molecules, as we have shown by cycling samples between different temperatures and observing an evolution in the height of the peak.

The S_8 population is significant at all temperatures. However, the mass fraction of rings is very low in all polymerized samples, and molecular loops with more than 24 atoms are exceptional and statistically irrelevant. With decreasing T, the relative fraction of rings other than S_8 increases from 3.0% at $T = 750$ K to 4.6% at $T = 550$ K.

Both molecular and polymeric samples display an almost linear dependence of density on temperature, but the polymer phase is characterized by a lower thermal expansion co-efficients. The crossing of the two $\rho(T)$ lines at $T_f = 433 \pm 10$ K provides an estimate of the polymerization temperature for the model.

The mean square distance between the two opposite chain heads grows linearly with the chain length over the entire polymer range, as expected for a Gaussian conformation. The radial distribution function is little affected by polymerization, but the third peak changes substantially, as found experimentally.[7,8]

3.4 Estimate of the polymerization temperature

Although the present simulations cannot reach equilibrium at temperatures close to the expected polymerization point ($400 \leq T \leq 450$), simulations at higher T provide sufficient
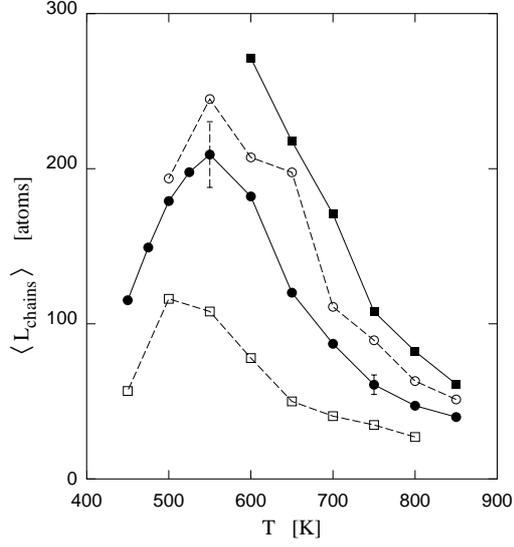
Figure 7. Average length of polymeric molecules as a function of T. Empty squares: $\Delta E_b = 15$ kcal/mol; solid dots: $\Delta E_b = 18$ kcal/mol; empty circles: $\Delta E_b = 20$ kcal/mol; filled squares: $\Delta E_b = 21$ kcal/mol. Representative error bars are shown. Lines are a guide to the eye.
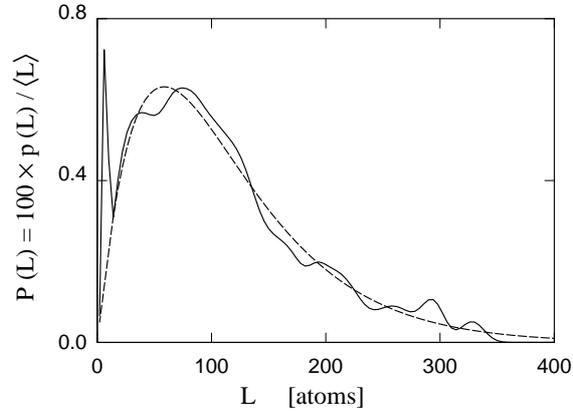

Figure 8. Mass fraction distribution function $P(L)$ for $T = 800$ K and $\Delta E_b = 21$ kcal/mol. Full curve: simulation results; dashed curve: interpolation by a Zimm-Schulz distribution excluding the peak at $L = 8$.

data for an extrapolation to this range. The simulation data for $\langle L \rangle(T)$ are reproduced fairly well by the simple analytic function:

$$\langle L \rangle(T) = [A(T - T_p) + B(T - T_p)^2] \exp(-\alpha T) \tag{3}$$

8

and T_p can be considered an estimate of the polymerization temperature T_f. The results of the fit ($T_p = 430$ K, 452 K, 455 K and 457 K for $\Delta E_b = 15, 18, 20$ and 21 kcal/mol) show a weak dependence of T_p on ΔE_b for $\Delta E_b \geq 18$ kcal/mol, thus allowing us to identify $T_p = 460$ K as the polymerization temperature T_f of the model in the limit of large ΔE_b.

For each value of ΔE_b, the linear term in the pre-exponential factor of Eq. (3) dominates, implying that the fit is continuous at T_p, but with a discontinuous first derivative. This is based on an extrapolation and cannot be a firm assignment of the nature of the transition. However, the results for the density $\rho(T)$ of the molecular and polymer phases cross at 435 K, and at $T = 460$ K they differ by less that 0.3%. Any discontinuity of $\rho(T)$ at the transition is very small, and the first derivative $d\rho(T)/dT$ is discontinuous at T_f.

The saturation of $N_{24}(T)$ at ~ 85 % of the total mass over a wide temperature range makes it difficult to fit its ΔE_b and T dependence with a simple analytic form. However, using the form of Eq. (3) and accepting a somewhat higher χ^2, we obtained results equivalent to those provided by $\langle L \rangle(T)$, with an estimate of the transition temperature of 450 K. The complexity of the fit and the extrapolation make it difficult to assign an error bar to these estimates. If the scatter of the three independent estimates of T_p obtained by: (a) fitting $\langle L \rangle(T)$ ($T_p = 460$ K), (b) fitting $N_{24}(T)$ ($T_p = 450$ K), and (c) plotting the densities of the molecular and of the polymer phase ($T_p = 433$ K) is a measure of the uncertainty in the determination of T_p, the polymerization temperature is estimated to be $T_f = 450 \pm 20$ K.

4   Discussion

The equilibrium polymerization of liquid sulphur has been investigated by Monte Carlo simulations. The interatomic potential consists of a flexible intramolecular contribution and a Lennard-Jones intermolecular part, and the parameters have been determined by fitting the results of density functional (DF) computations for small sulphur rings and chains.[9] The potential energy scheme goes beyond earlier work on sulphur by allowing the breaking and formation of covalent bonds, and the parameter ΔE_b represents the energy cost of breaking a bond, or energy gain upon forming a new one. Bond breaking and formation allow the system to approach equilibrium with respect to the bond configuration. The kinetics of bond equilibration is strongly enhanced by introducing a further relaxation mechanism, corresponding to bond interchanges around unsaturated chain terminations, following the pattern illustrated in Fig. 3.

The equilibrium concentration of unsaturated atoms in the liquid phase is proportional to the exponential of $[-\Delta E_b/2k_BT]$, which prevents the present simulations from reaching equilibrium for values of ΔE_b near the DF (25 kcal/mol) or experimental ($32 - 36$ kcal/mol) estimates. Nevertheless, equilibrium is reached over a domain of ΔE_b and T sufficiently wide to allow the investigation of the polymer phase and the dependence of the results on ΔE_b ($T \geq 450$ K for $\Delta E_b = 15$ kcal/mol, $T \geq 500$ K for $\Delta E_b = 18$ kcal/mol, $T \geq 550$ K for $\Delta E_b = 20$ and $T \geq 600$ K for $\Delta E_b = 21$ kcal/mol). Above these temperatures (the highest simulation temperature was $T = 850$ K), liquid samples comprising S_8 molecules polymerize when the system is allowed to relax its bond configuration.

Polymerization is accompanied by an enthalpy increase ΔH, thus confirming that polymerization is entropy driven. Simple considerations show that translational entropy opposes polymerization, while vibrational entropy is nearly unchanged across the transition.

By analogy to earlier model calculations,[10,11] this suggests that polymerization is due to the entropy associated to the distribution of bonds among sulphur atoms. The polymer co-exists in all samples with a significant population of S_8 molecules, whose relative weight increases rapidly with decreasing T. The molecular size distribution function for all other species follows a Zimm-Schulz distribution, whose parameters depend in a predictable way on ΔE_b and T. Molecules with more than 24 atoms are almost always open chains, and the concentration of rings other than S_8 is low at all T.

The thermal expansion coefficient of the polymer phase is lower than that of the liquid comprising S_8 molecules alone. The temperature dependence of the density in each is approximately linear over a wide temperature range, and the linear interpolations for the two data sets cross at $T = 433 \pm 10$ K. This point depends only slightly on ΔE_b. Assuming that the temperature dependence of the density is continuous across the transition, and that only its slope $d\rho(T)/dT$ (directly related to the thermal expansion coefficient) changes discontinuously, this point ($T = 433 \pm 10$ K) is our first estimate for the polymerization temperature of the model. Independent estimates are obtained by fitting the temperature dependence of the average chain length ($T_f = 460$ K), and of the polymerized fraction N_{24} ($T_f = 450$ K). From these three values, which are based on the assumption that the variable is continuous across the transition, with a discontinuous first derivative with respect to T, we predict a polymerization temperature $T_f = 450 \pm 20$ K.

Acknowledgments

References

1. J. Donohue, *The Structure of the Elements* (Wiley, New York, 1974), Chap. 9.
2. R. Steudel, Top. Curr. Chem. **230** (2003) [in press].
3. S. C. Greer, Annu. Rev. Phys. Chem. **53**, 173 (2002).
4. A. V. Tobolsky and A. Eisenberg, J. Am. Chem. Soc. **81**, 780 (1959).
5. R. Steudel, Phosphorus and Sulfur **16**, 251 (1983); R. Steudel, S. Passlack-Stephan, and G. Holdt, Z. anorg. allg. Chem. **517**, 7 (1984).
6. F. H. Stillinger, T. A. Weber, and R. A. LaViolette, J. Chem. Phys. **85**, 6460 (1986).
7. R. Winter, C. Szornel, W. C. Pilgrim, W. S. Howells, and P. A. Egelstaff, T. Bodensteiner, J. Phys. Condens. Matter **2**, 8427 (1990); M. Stolz, R. Winter, W. S. Howells, R. L. McGreevy, and P. A. Egelstaff, J. Phys. Condens. Matter **6**, 3619 (1994).
8. R. Bellissent, L. Descotes, F. Boué, and P. Pfeuty, Phys. Rev. B **41**, 2135 (1990).
9. R. O. Jones and P. Ballone, J. Chem. Phys. **118**, 9257 (2003).
10. P. Ballone and R. O. Jones, J. Chem. Phys. **115**, 3895 (2001).
11. P. Ballone and R. O. Jones, J. Chem. Phys. **116**, 7724 (2002).